University of Texas Rio Grande Valley

ScholarWorks @ UTRGV

Physics and Astronomy Faculty Publications
and Presentations

College of Sciences

Upper bounds on the low-frequency stochastic gravitational wave background from pulsar timing observations: Current limits and future prospects

F. A. Jenet

G. B. Hobbs

W. Van Straten

R. N. Manchester

M. Bailes

See next page for additional authors

Follow this and additional works at: https://scholarworks.utrgv.edu/pa_fac

Part of the Astrophysics and Astronomy Commons

Recommended Citation

Authors

F. A. Jenet, G. B. Hobbs, W. Van Straten, R. N. Manchester, M. Bailes, J. P.W. Verbiest, R. T. Edwards, A. W. Hotan, J. M. Sarkissian, and S. M. Ord

UPPER BOUNDS ON THE LOW-FREQUENCY STOCHASTIC GRAVITATIONAL WAVE BACKGROUND FROM PULSAR TIMING OBSERVATIONS: CURRENT LIMITS AND FUTURE PROSPECTS

F. A. JENET,[1] G. B. HOBBS,[2] W. VAN STRATEN,[1] R. N. MANCHESTER,[2] M. BAILES,[3] J. P. W. VERBIEST,[2,3]
R. T. EDWARDS,[2] A. W. HOTAN,[4] J. M. SARKISSIAN,[2] AND S. M. ORD[5]

ABSTRACT

Using a statistically rigorous analysis method, we place limits on the existence of an isotropic stochastic gravitational wave background using pulsar timing observations. We consider backgrounds whose characteristic strain spectra may be described as a power-law dependence with frequency. Such backgrounds include an astrophysical background produced by coalescing supermassive black-hole binary systems and cosmological backgrounds due to relic gravitational waves and cosmic strings. Using the best available data, we obtain an upper limit on the energy density per unit logarithmic frequency interval of $\Omega_g^{\mathrm{SMBH}}[1/(8\ \mathrm{yr})]h^2 \leq 1.9 \times 10^{-8}$ for an astrophysical background that is 5 times more stringent than the earlier limit of 1.1×10^{-7} found by Kaspi and colleagues. We also provide limits on a background due to relic gravitational waves and cosmic strings of $\Omega_g^{\mathrm{relic}}[1/(8\ \mathrm{yr})]h^2 \leq 2.0 \times 10^{-8}$ and $\Omega_g^{\mathrm{cs}}[1/(8\ \mathrm{yr})]h^2 \leq 1.9 \times 10^{-8}$, respectively. All of the quoted upper limits correspond to a 0.1% false alarm rate together with a 95% detection rate. We discuss the physical implications of these results and highlight the future possibilities of the Parkes Pulsar Timing Array project. We find that our current results can (1) constrain the merger rate of supermassive binary black hole systems at high redshift, (2) rule out some relationships between the black hole mass and the galactic halo mass, (3) constrain the rate of expansion in the inflationary era, and (4) provide an upper bound on the dimensionless tension of a cosmic string background.

Subject headings: gravitational waves — pulsars: general

1. INTRODUCTION

Pulsar timing observations (see Lorimer & Kramer [2005] and Edwards et al. [2006] for a review of the techniques) provide a unique opportunity to study low-frequency (10^{-9} to 10^{-7} Hz) gravitational waves (GWs; e.g., Sazhin 1978; Detweiler 1979; Bertotti et al. 1983; Foster & Backer 1990; Kaspi et al. 1994; Jenet et al. 2005). Sources in this low-frequency band include binary supermassive black holes, cosmic superstrings, and relic gravitational waves from the big bang (Jaffe & Backer 2003; Maggiore 2000).

An isotropic stochastic background can be described by its characteristic strain spectrum $h_c(f)$, which, for most models of interest, can be written as a power-law dependence on frequency, f:

$$h_c(f) = A\left(\frac{f}{\mathrm{yr}^{-1}}\right)^{\alpha}. \tag{1}$$

Table 1 shows the expected values of A and α for different types of stochastic backgrounds that have been addressed in the literature. The characteristic strain is related to the one-sided power spectrum of the induced timing residuals, $P(f)$, as

$$P(f) = \frac{1}{12\pi^2}\frac{1}{f^3}h_c(f)^2, \tag{2}$$

and to $\Omega_{\mathrm{gw}}(f)$, the energy density of the background per unit logarithmic frequency interval, as

$$\Omega_{\mathrm{gw}}(f) = \frac{2}{3}\frac{\pi^2}{H_0^2}f^2 h_c(f)^2, \tag{3}$$

where H_0 is the Hubble constant. Note that the one-sided power spectrum, $P(f)$, is defined so that

$$\int_0^{\infty} P(f)df = \sigma^2, \tag{4}$$

where σ^2 is the variance of the arrival time fluctuations, or timing residuals, generated by the presence of the GW background. Since σ^2 has the physical units of s², $P(f)$ has the units of s² Hz⁻¹, or s³.

Jenet et al. (2005) developed a technique to make a definitive detection of a stochastic background of GWs by looking for correlations between pulsar observations. It was shown that approximately 20 pulsars would need to be observed with a timing precision of ~100 ns over a period of 5 years in order to make such a detection if the GW background is at the currently predicted level (Jaffe & Backer 2003; Wyithe & Loeb 2003; Enoki et al. 2004; Sesana et al. 2004). The Parkes Pulsar Timing Array (PPTA) project (Hobbs 2005) is trying to achieve these ambitious goals, but the currently available data sets do not provide the required sensitivity for a detection. In this paper, we introduce a method to place an upper bound on the power of a specified stochastic GW background, using observations of multiple pulsars. Full technical details of our implementation will be published in G. B. Hobbs et al. (2007, in preparation). Here, this method is applied to data (see § 2) from seven pulsars observed for the PPTA project combined with an earlier publicly available data set.

[1] Center for Gravitational Wave Astronomy, University of Texas, Brownsville, TX 78520; merlyn@phys.utb.edu.

[2] Australia Telescope National Facility, CSIRO, P.O. Box 76, Epping, NSW 1710, Australia.

[3] Centre for Astrophysics and Supercomputing, Swinburne University of Technology, P.O. Box 218, Hawthorn, VIC 3122, Australia.

[4] Physics Department, University of Tasmania, Hobart, TAS 7001, Australia.

[5] School of Physics, University of Sydney, NSW 2006, Australia.

TABLE 1
EXPECTED PARAMETERS FOR PREDICTED STOCHASTIC BACKGROUNDS

Model	A	α	References
Supermassive black holes......	10^{-15} to 10^{-14}	$-2/3$	Jaffe & Backer (2003), Wyithe & Loeb (2003), Enoki et al. (2004)
Relic GWs............................	10^{-17} to 10^{-15}	-1 to -0.8	Grishchuk (2005)
Cosmic string	10^{-16} to 10^{-14}	$-7/6$	Maggiore (2000)

Upper limits have already been placed on the amplitude of any such background of GWs. Using 8 years of observations for PSR B1855+09, Kaspi et al. (1994) obtained a limit of $\Omega_g h^2 \leq 1.1 \times 10^{-7}$, where $H_0 = 100\ h$ km s^{-1} Mpc^{-1}, at the 95% confidence level[6] for the case when $\alpha = -1$ (i.e., Ω_{gw} is independent of frequency). This work was continued by Lommen (2002), who used 17 years of observations to obtain $\Omega_g h^2 < 2 \times 10^{-9}$. However, the statistical method used for both of these analyses has been criticized in the literature (see, for instance, Thorsett & Dewey 1996; McHugh et al. 1996; Damour & Vilenkin 2005). In this paper, we develop a frequentist technique, similar to that used by the LIGO science collaboration (Abbott et al. 2006), to place an upper bound on A, given α. The technique makes use of a statistic, Υ, defined below, that is sensitive to red noise in the pulsar timing residual data. Upper bounds on A are determined using Υ together with a specified false alarm rate, $\mathcal{P}_f$, and detection rate, $\mathcal{P}_d$. Monte Carlo simulations are used to determine these probabilities by generating pulsar pulse times of arrival consistent with a GW background. All of the upper limits quoted in this paper correspond to $\mathcal{P}_f = 0.1\%$ and $\mathcal{P}_d = 95\%$.

2. OBSERVATIONS

We expect the isotropic background to generate timing residuals with a "red" spectrum: a spectrum with excess power at low frequencies or, equivalently, long-timescale correlations in the residuals. Therefore, we have restricted our analysis to those pulsars having formally white spectra: a spectrum with statistically equal power at all frequencies or no correlations in the residuals. This allows us to put the best upper limit on the background by bounding the level of any red process in those data sets. Three separate tests were used in order to determine the statistical properties of the data and to select data sets that are statistically white. First, the normalized Lomb-Scargle periodogram was calculated for each residual time series. No significant peaks were seen in any of the data used. Second, the variance of the residuals was shown to decrease as $1/n$, where n is the number of adjacent time samples averaged together. If the data were correlated, the variance would not scale as $1/n$. Third, no significant structures were seen in the polynomial spectrum (defined below) for each individual spectrum or in the averaged spectra. Note that the publicly available data set for PSR B1937+21 (Kaspi et al. 1994) was not used in our analysis, since its timing residuals do not pass these three tests.

We made use of the following data sets, which passed the tests: (1) observations of PSR B1855+09 (also known as PSR J1857+0943) from the Arecibo radio telescope that are publicly available (Kaspi et al. 1994); (2) observations for PSRs B1855+09, J0437−4715, J1024−0719, J1713+0747, J1744−1134, J1909−3744, and B1937+21 (J1939+2134) using the Parkes radio telescope and reported by Hotan et al. (2006); and (3) recent observations of all

of these pulsars made as part of the PPTA and related Swinburne timing projects. The Kaspi et al. (1994) data set was obtained at ~1400 MHz over a period of 8 years. The PPTA observations, which commenced in 2004 February, include ~20 millisecond pulsars and use the 10/50 cm dual-frequency receiver and a 20 cm receiver at the Parkes radio telescope. Each pulsar is typically observed at all three frequencies in sessions at intervals of 2–3 weeks. The results used here were obtained using a correlator with 2 bit sampling capable of bandwidths up to 1 GHz and a digital filterbank system with 8 bit sampling of a 256 MHz bandwidth. The PPTA observations and the earlier Hotan et al. (2006) data sets also used the Caltech Parkes Swinburne Recorder 2 (CPSR2; see Hotan et al. 2006), a baseband recorder that coherently dedisperses two observing bands of 64 MHz bandwidth, centered on 1341 and 1405 MHz for observations at 20 cm and around 3100 and 685 MHz for (simultaneous) observations with the coaxial 10/50 cm receiver. Full details of the PPTA project will be presented in a forthcoming paper; up-to-date information can be obtained from our Web site.[7] Unfortunately, our stringent requirements on the "whiteness" of the timing residuals has restricted the use of some of our nominally best-timing pulsars. For instance, even though a 10 yr data span is available for PSR J0437−4715, the full-length data set is significantly affected by calibration and hardware-induced artifacts, as well as other unknown sources of timing noise.

A listing of the pulsars observed, the observation span, number of points, and weighted rms timing residual after fitting for the pulsars' pulse frequency and its first derivative, astrometric, and binary parameters are presented in Table 2. Arbitrary offsets have been subtracted between data sets obtained with different instrumentation. Combining these data sets provides us with data spans of ~20 yr for PSR B1855+09 and ~2–4 yr for the remaining pulsars. The final timing residuals are plotted in Figure 1.

3. NEW UPPER BOUNDS ON THE STOCHASTIC BACKGROUNDS

The goal here is to use the measured timing residuals from multiple pulsars in order to determine the smallest value of A that can be detected for a given α, as defined by equation (1). This is done in a three-step process. First, a detection algorithm is defined

[7] See http://www.atnf.csiro.au/research/pulsar/ppta.

---

[6] Their more stringent constraint of $\Omega_g h^2 \leq 6 \times 10^{-8}$ was obtained when data from PSRs B1855+09 and B1937+21 were combined. Since the data from PSR B1937+21 is far from white, we believe this limit is artificially low and therefore restrict our discussion to the PSR B1855+09 data only.

TABLE 2
PULSAR OBSERVATIONS USED FOR THIS ANALYSIS

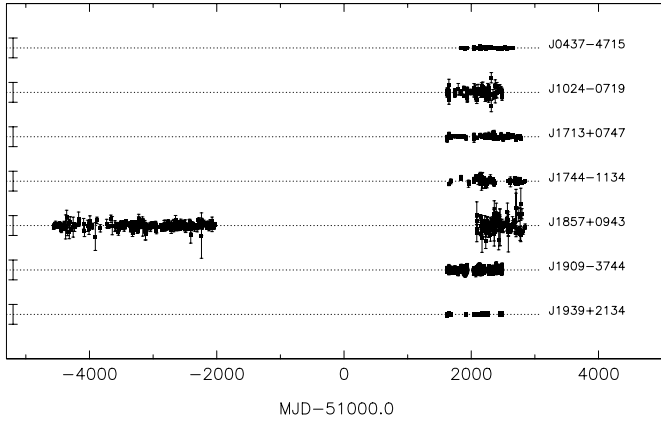| Pulsar	Telescope	Span (days)	N	rms Residual (μs)
J0437−4715.........	Parkes	815	233	0.12
J1024−0719.........	Parkes	861	92	1.10
J1713+0747..........	Parkes	1156	168	0.23
J1744−1134.........	Parkes	1198	101	0.52
J1857+0943..........	Arecibo/Parkes	7410	398	1.12
J1909−3744..........	Parkes	866	2859	0.29
J1939+2134..........	Parkes	862	231	0.21

FIG. 1.—Pulsar timing residuals. The length of the vertical line on the left-hand side represents 10 μs.

that is sensitive to the presence of the background. Second, this algorithm is tuned so that in the absence of a signal (i.e., $A = 0$), the probability of the detection scheme falsely detecting the background is set at $\mathcal{P}_f$, known as the false alarm rate. Lastly, for the given detection scheme and false alarm rate, the upper bound, A_{up}, is chosen so that the probability of detecting a background with $A = A_{up}$ is $\mathcal{P}_d$. For this paper, the false alarm rate is set to 0.1%, while the upper bound detection rate is set to 95%.

Since all current models of the background predict that the induced timing residuals will be red (the spectrum increases at lower frequencies), the detection scheme employed here is defined to be sensitive to a red spectrum. The existence of a red spectrum in the timing residuals is therefore necessary, but not sufficient, evidence for the existence of a GW background. Hence, we can use a statistic sensitive to a red spectrum in order to place an upper bound on the amplitude of the characteristic strain spectrum. Since the data sets are irregularly sampled and cover different time spans, a spectrum based on orthogonal polynomials is employed. Each pulsar data set consists of n_p measured residuals, $x_p(i)$, a time tag $t_p(i)$, and an uncertainty $\sigma_p(i)$, where i is the data sample index and p is an index referring to a particular pulsar. The time tags are scaled so that normalized time tags, $\tau_p(i)$, run from -1 to 1.

These $\tau_p(i)$ values are used in a weighted Gram-Schmidt orthogonalization procedure to determine a set of orthonormal polynomials, $j_p^l(i)$, defined from

$$\sum_{i=0}^{n_p-1} \frac{j_p^l(i)j_p^k(i)}{\sigma_p^2(i)} = \delta_{lk}, \tag{5}$$

where $j_p^l(i)$ is the lth order polynomial evaluated at $\tau_p(i)$ and δ_{lk} is the standard Kronecker delta function. Note that the highest power of t in $j_p^l(i)$ is l. For the case when τ is continuous and $\sigma_p^2(i) = 1$, the above sum becomes an integral and $j_p^l(i)$ become the familiar Legendre polynomials. The following coefficients are calculated using the orthonormal polynomials, $j_p^l(i)$, and the timing residuals, $x_p(i)$:

$$C_p^l = \sum_{i=0}^{n_p-1} \frac{j_p^l(i)x_p(i)}{\sigma_p^2(i)}. \tag{6}$$

The pulsar average polynomial spectrum is given by

$$P_l = \sum_p \frac{(C_p^l)^2}{v_p}, \tag{7}$$

where the weighted variance, v_p, is defined as $(1/n_p)\sum_{i=0}^{n_p-1}[x_p(i) - \bar{x}_p]^2/\sigma_p^2(i)$ and $\bar{x}$ is the mean of x. Since the stochastic background is red, P_l will be large for low values of l if the background significantly influenced the residuals. Hence, $\Upsilon = \sum_{l=0}^{l=7} P_l$ can be used as a statistic to detect the background. An upper limit of $l = 7$ is used, since 95% of the power is contained in the first seven polynomials for the case of $\alpha = -2/3$. The background will be "detected" if $\Upsilon > \Upsilon_0$, where Υ_0 is set so that the false-alarm rate is given by $\mathcal{P}_f$.

A Monte Carlo simulation was used to determine Υ_0 and A_{up}. Complete details of the simulation and its implementation may be found in G. B. Hobbs et al. (2007, in preparation), but a brief overview is given here. The simulation, undertaken in the pulsar timing package TEMPO2 (G. B. Hobbs et al. 2007, in preparation), generates an ideal time of arrival (TOA) data set (with the same sampling as the observed data) from a measured set of TOAs and a given timing model. The fluctuations due to the GW background for a given A and α are introduced into the TOAs by adding together 10,000 sinusoidal GWs, which come from random directions on the sky and have randomly chosen frequencies in the range $1/(2000 \text{ yr})$–$1/(0.5 \text{ days})$. As a test of the simulation, the ensemble-averaged power spectrum of the simulated residuals was calculated over a timescale much larger then the longest GW timescale (i.e., 2000 yr) and was shown to be consistent with equation (2), as expected. The GW residuals are then added to the ideal TOA data set for each pulsar. In order to include the effects of measurement noise, the measured timing residuals are added back into the data set, but randomly shuffled. This ensures that the added noise has the same probability distribution as the actual measurement noise. In this way, a new set of TOAs are generated that include both measurement noise and the GW background. Note that the shuffling procedure is only valid when the data have a white spectrum. Otherwise, the spectral properties of the original data set and the shuffled data set will not be the same. This simulated TOA data set will then be analyzed in exactly the same way as a real data set. Hence, all the systemic effects that inhibit gravitational wave detection, such as low order polynomial removal, Earth's orbital motion, annual parallax effects, and orbital companion effects, are appropriately accounted for in the simulation.

To calculate Υ_0, the simulation generates 10,000 independent simulated sets of TOAs for each pulsar with $A = 0$ (i.e., no GW background). The statistic Υ is calculated for each of the 10,000 trials. Using this set of Υ values, together with the chosen false alarm rate, $\mathcal{P}_f$, the value of Υ_0 can be determined. Once Υ_0 is chosen, the simulation is used to generate TOA data sets that include the effects of GWs. For a given value of A, the probability of detection is determined using Υ and Υ_0. A_{up} is chosen to be that value of A when the probability of detection is equal to $\mathcal{P}_d$.

Note that the effects of unknown time offsets ("jumps") in the data sets are included in the calculation of both Υ_0 and A_{up} using this technique, since TEMPO2 fits for these offsets in the TOA data set after the GW background has been added. Since we are using TEMPO2 to analyze the data, the effects of all the fitting procedures are being taken into account.

4. RESULTS

Using the pulsar data sets described above, the 95% detection rate upper bound with a false alarm rate of 0.1% is given in Table 3 for different values of α. The relationship between A and α is shown in Figure 2. These upper bounds on A can be converted to an upper bound on the normalized GW energy density per unit logarithmic frequency interval, $\Omega_{gw}(f)$, using equations (1) and (3). Our limits on $\Omega_{gw}(1 \text{ yr}^{-1})$ are indicated on the right-hand axis of Figure 2.

α	A	$\Omega_{gw}[1/(1\ \mathrm{yr})]h^2$	$\Omega_{gw}[1/(8\ \mathrm{yr})]h^2$	$\Omega_{gw}[1/(20\ \mathrm{yr})]h^2$
$-2/3$	1.1×10^{-14}	7.6×10^{-8}	1.9×10^{-8}	1.0×10^{-8}
-1	5.7×10^{-15}	2.0×10^{-8}	2.0×10^{-8}	2.0×10^{-8}
$-7/6$	3.9×10^{-15}	9.6×10^{-9}	1.9×10^{-8}	2.6×10^{-8}
$-2/3$	6.5×10^{-16}	2.7×10^{-10}	6.6×10^{-11}	3.6×10^{-11}
-1	3.8×10^{-16}	9.1×10^{-11}	9.1×10^{-11}	9.1×10^{-11}
$-7/6$	2.8×10^{-16}	4.9×10^{-11}	9.9×10^{-11}	1.3×10^{-10}

NOTES.—The first three rows give limits derived from current observations. Limits based on timing 20 pulsars with an rms timing residual of 100 ns over 5 yr are given in the last three rows.

We can compare our results to the previously published limit of Kaspi et al. (1994), who obtained $\Omega_{gw}[1/(8\ \mathrm{yr})]h^2 < 1.1 \times 10^{-7}$ (star symbol in Fig. 2). Using the same data set as Kaspi et al. (1994), our method provides a similar limit of $\Omega_{gw}[1/(8\ \mathrm{yr})]h^2 < 1.3 \times 10^{-7}$. Combining this data set with our more recent observations provides a more stringent limit of $\Omega_{gw}[1/(8\ \mathrm{yr})]h^2 < 1.9 \times 10^{-8}$.

The most stringent limit reported to date was obtained by Lommen (2002). Unfortunately, these observations are not publicly available. In order to compare our technique, we use the original PSR B1855+09 Kaspi et al. (1994) data set along with two simulated white data sets that realistically model the NRAO 140 foot telescope and Arecibo observations that form the remainder of the Lommen (2002) data (we simulate 60 observations with an rms residual of 5 μs between MJDs 47800 and 51360 for the 140 foot telescope and a further 60 observations with an rms residual of 1 μs between MJDs 50783 and 52609 for the most recent Arecibo data). As we simulate neither systematic effects nor timing noise, our limit will be more stringent than could be obtainable using the real data set. For $\alpha = -2/3$, we obtained $A \leq 9 \times 10^{-15}$, corresponding to $\Omega_{gw}[1/(17\ \mathrm{yr})]h^2 = 8 \times 10^{-9}$. This limit is a factor of 4 less stringent than that reported by Lommen (2002).

Using simulated data, the upper bounds that can be expected from future experiments can be determined. The goal of the PPTA is to time 20 pulsars with an rms timing residual of 100 ns over 5 years. The dashed line in Figure 2 plots A versus α for such a data set, which could potentially provide a limit on a background of supermassive black hole systems of $A_{up} < 6.5 \times 10^{-16}$ or $\Omega_{gw}[1/(8\ \mathrm{yr})]h^2 \leq 6.6 \times 10^{-11}$ (see Table 3).

In Jenet et al. (2005), techniques to use an array of pulsars to detect a stochastic background of GWs with $\alpha = -2/3$ were developed.[8] Given a value for A_{up}, one can use such techniques to determine the probability of definitively detecting the GW background using the completed PPTA data sets (20 pulsars with an rms timing residual of 100 ns over 5 years) if A were equal to A_{up}. In terms of the parameter S, defined in Jenet et al. (2005), a significant detection would occur if $S > 3.1$. This corresponds to a 0.001 false alarm rate. For the case of $\alpha = -2/3$, the expected value of S (assuming ideal whitening) is about 4.1 for $A = A_{up}$. Since the probability distribution of S is approximately Gaussian, the probability of $S > 3.1$ when $\langle S \rangle = 4.1$ is 85%. Hence, the GW background would be detected 85% of the time. For the case of 10 years of observations, the detection rate increases to over 99% of the time.

---

[8] Note that A, as defined here, is larger by a factor of $\sqrt{3}$ compared to the definition of A used in Jenet et al. (2005). The definition used here is consistent with Jaffe & Backer (2003) and Wyithe & Loeb (2003).
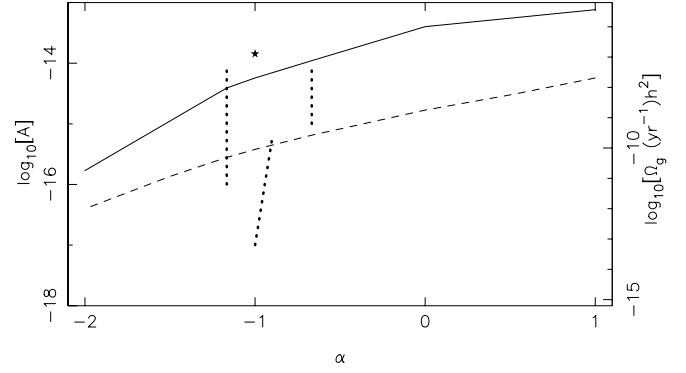

FIG. 2.—Minimum detectable A [or $\Omega_{gw}(1\ \mathrm{yr}^{-1})\ h^2$; *right axis*] vs. α for our current limits (*solid line*) and potential future limits from the PPTA (*dashed line*). The star symbol indicates the limit obtainable using the Kaspi et al. (1994) observations of PSR B1855+09. From left to right, the near-vertical dotted lines indicate the expected range of amplitudes for the cosmic strings, relic GW, and supermassive black hole background, respectively.

5. IMPLICATIONS AND DISCUSSION

The upper bound on the stochastic background can be used to probe several aspects of the universe. Precisely what is being constrained depends on the physics of the particular background in question. Here, both the measured upper bounds using the currently available data and the expected upper bounds using the full 5 year PPTA data set are discussed in the context of several GW backgrounds.

5.1. Supermassive Black Holes

A GW background generated by an ensemble of supermassive black holes distributed throughout the universe has been investigated by several authors (Jaffe & Backer 2003; Wyithe & Loeb 2003; Enoki et al. 2004). In general, the characteristic strain spectrum for this background can be written as:

$$h_c(f) = 2.5 10^{-16} h \left(\frac{f}{\mathrm{yr}^{-1}} \right)^{-2/3} \left\langle \left(\frac{M_c}{10^7\ M_\odot} \right)^{5/3} \right\rangle^{1/2} \left(\frac{N_0}{\mathrm{Mpc}^{-3}} \right)^{1/2} I^{1/2},$$

(8)

where

$$I = \int \frac{N(z)}{N_0} H_0 \frac{a(z)}{\dot{a}(z)} \frac{dz}{(1+z)^{4/3}},$$

(9)

$a(z)$ is the cosmological scale factor written in terms of redshift, z, $\dot{a}(z)$ is the derivative of $a(z)$ with respect to cosmic time, H_0 is the Hubble constant, the chirp mass $M_c = [M_1 M_2 (M_1 + M_2)^{-1/3}]^{3/5}$ of a given binary system, $\langle \cdots \rangle$ represents ensemble averaging over all the systems generating the background, $N(z)$ is the galaxy merger rate as a function of redshift, and N_0 is the present-day number density of merged galaxies that created a black hole binary system. The values of each of these physical quantities are currently poorly constrained, and each investigator has chosen a different parameterization. Under the framework described by Jaffe & Backer (2003), $\langle M_c^{5/3} \rangle$ and N_0 are constrained by observations at the current epoch to be $\langle M_c \rangle \approx 2.3 \times 10^7\ M_\odot$ and $N_0 \approx 1\ \mathrm{Mpc}^{-3}$. They parameterized the galaxy merger rate such that $R(z)$ goes as $(1+z)^\gamma$. Hence, I depends on γ. Combining the estimates of $\langle M_c \rangle$ and N_0 with our measured upper

bound of $A_{up} = 1.1 \times 10^{-14}$, one finds that $I \leq 3$. Using the full PPTA after 5 years, one expects $I \leq 0.8$. These constraints, together with the calculations of Jaffe & Backer (2003; see Fig. 4 in their work), constrain γ. Currently, the limit on γ is <2.6 and with the full PPTA $\gamma < 0.4$. This value is expected to lie somewhere between -0.4 and 2.3 (Carlberg et al. 2000; Patton et al. 2002). Current PPTA sensitivity (i.e., using the data presented in this paper) is just above the expected range, while the full PPTA should be able to place meaningful constraints on this exponent.

In the Wyithe & Loeb (2003) work, both $\langle M_c^{5/3} \rangle$ and I depend strongly on the black hole versus galactic-halo mass (M_{BH}-M_{HM}) relationship. They discuss several different scenarios, which yield different M_{BH}-M_{HM} relationships, and hence different levels of the background. For the case of an M_{BH}-M_{HM} relationship determined by Ferrarese (2002), the expected value of A is 2×10^{-15}. For the M_{BH}-M_{HM} relationship derived from Navarro et al. (1997), $A = 5 \times 10^{-15}$. Using an M_{BH}-M_{HM} relationship derived from simple considerations of black hole growth by feedback from quasar activity (Wyithe & Loeb 2003; Haehnelt et al. 1998; Silk & Rees 1998), $A \approx 10^{-15}$. Our measured upper limit for $\alpha = -2/3$ cannot rule out any of these models. However, if only a limit is obtained from the full PPTA observations, it will rule out all of the models described above.

5.2. Relic Gravitational Waves

A relic GW background is generated by the interaction between the large-scale dynamic cosmological metric and quantum fluctuations of the metric perturbations occurring in the early universe (Grishchuk 2005). In the nHz frequency regime, the background takes the following form:

$$h_c(f) = h_c(f_h)\left(\frac{f}{H_0}\right)^{\alpha}\left(\frac{a_2}{a_H}\right)^{1/2}, \qquad (10)$$

where $h_c(f_h)$ is the magnitude of the characteristic strain spectrum at $f = H_0$, a_H is the current value of the cosmological expansion factor, and a_2 is the value of the expansion factor at the start of the matter-dominated epoch. Note that this expression is not valid in the ultralow frequency regime where $f \approx H_0$. The notation used here is consistent with Grishchuk (2005), except for α, which is related to Grishchuk's parameter β by $\alpha = 1 + \beta$. The exponent determines the evolution of the inflationary epoch that starts the GW amplification process. When $\alpha = -1$, the scale factor grows exponentially with global cosmic time. The ratio a_2/a_H is believed to be about 10^{-4}. The $h_c(f_h)$ value is constrained by cosmic microwave background measurements to be about 10^{-5}. Using these values and assuming the validity of the amplification scenario described in Grishchuk (2005), the upper bound on A may be used to constrain α. The upper bound on α is given by the solution to the following equation:

$$h_c(f_h)\left[\frac{1/(1\ \mathrm{yr})}{f_h}\right]^{\alpha}\left(\frac{a_2}{a_H}\right)^{1/2} = A(\alpha). \qquad (11)$$

The above equation yields $\alpha \leq -0.7$ for the current PPTA and $\alpha \leq -0.84$ for the full PPTA. Within the theoretical framework described by Grishchuk (2005), if α is larger than -0.80, small-scale GWs will affect primordial nucleosynthesis, while an α less than -1.0 will result in an infinitely large energy density in small-scale GWs. Hence, the full PPTA will be able to place useful constraints on the relic GW background. Since α determines the

rate of expansion in the inflationary epoch, it turns out that it is related to the equation of state of the "matter" in that epoch by

$$\frac{P}{\epsilon} = w = \frac{2 - \alpha}{3\alpha}, \qquad (12)$$

where P is the pressure and ϵ the energy density. The full PPTA will constrain w in the early universe to be greater than -1.17. This would limit inflationary models based on "quintessence" and "phantom energy" (Nojiri et al. 2006; Padmanabhan 2005).

5.3. Cosmic Strings

It has been proposed that oscillating cosmic string loops will produce GW radiation (Vilenkin 1981). Recently, Damour & Vilenkin (2005) discussed the possibility of generating a stochastic GW background using a network of cosmic superstrings. Using a semianalytical approach, they derived the following characteristic strain spectrum, valid in the pulsar timing frequency range (see their equation [4.8]):

$$h_c(f) = 1.6 \times 10^{-14} c^{1/2} p^{-1/2} \epsilon_{\mathrm{eff}}^{-1/6}$$
$$\times (h/0.65)^{7/6}\left(\frac{G\mu}{10^{-6}}\right)^{1/3}\left(\frac{f}{\mathrm{yr}^{-1}}\right)^{-7/6}, \qquad (13)$$

where μ is the string tension, G is Newton's constant, c is the average number of cusps per loop oscillation, p is the reconnection probability, ϵ_{eff} is a loop length scale factor, and h is the Hubble constant in units of 100 km s^{-1} Mpc^{-1}. Note that for the above estimate, h was evaluated at 0.65 in order to be consistent with Damour & Vilenkin (2005). The combination $G\mu$ is the dimensionless string tension that characterizes the gravitational interaction of the strings. The predicted string tensions are $10^{-11} \leq G\mu \leq 10^{-6}$ (Damour & Vilenkin 2005). Using the above spectrum, together with the measured upper bound on h_c for $\alpha = -7/6$, an upper bound can be placed on the dimensionless string tension:

$$G\mu \leq 1.5 \times 10^{-8} c^{-3/2} p^{3/2} \epsilon_{\mathrm{eff}}^{1/2}(h/0.65)^{-7/2}. \qquad (14)$$

As emphasized by Damour & Vilenkin (2005), the above expression for the upper bound may be simplified using the fact that both p and ϵ_{eff} are less than one and h is expected to be greater than 0.65:

$$G\mu \leq 1.5 \times 10^{-8} c^{-3/2}. \qquad (15)$$

Using a standard model assumption in which $c = 1$, the upper bound becomes $G\mu \leq 1.5 \times 10^{-8}$. This is already limiting the parameter space of the cosmic string model of Sarangi & Tye (2002). With the full PPTA, the limit will become $G\mu \leq 5.36 \times 10^{-12}$. Hence, the full PPTA will either detect GWs from cosmic strings or rule out most current models.

REFERENCES

Abbott, B., et al. 2006, Phys. Rev. D, 73, 062001
Bertotti, B., Carr, B. J., & Rees, M. J. 1983, MNRAS, 203, 945
Carlberg, R. G., et al. 2000, ApJ, 532, L1
Damour, T., & Vilenkin, A. 2005, Phys. Rev. D, 71, 063510
Detweiler, S. 1979, ApJ, 234, 1100
Edwards, R. T., Hobbs, G. B., & Manchester, R. N. 2006, MNRAS, 372, 1549
Enoki, M., Inoue, K. T., Nagashima, M., & Sugiyama, N. 2004, ApJ, 615, 19
Ferrarese, L. 2002, ApJ, 578, 90
Foster, R. S., & Backer, D. C. 1990, ApJ, 361, 300
Grishchuk, L. P. 2005, Phys. Uspekhi, 48, 1235
Haehnelt, M. G., Natarajan, P., & Rees, M. J. 1998, MNRAS, 300, 817
Hobbs, G. 2005, Publ. Astron. Soc. Australia, 22, 179
Hotan, A. W., Bailes, M., & Ord, S. M. 2006, MNRAS, 369, 1502
Jaffe, A. H., & Backer, D. C. 2003, ApJ, 583, 616
Jenet, F. A., Hobbs, G. B., Lee, K. J., & Manchester, R. N. 2005, ApJ, 625, L123
Kaspi, V. M., Taylor, J. H., & Ryba, M. 1994, ApJ, 428, 713
Lommen, A. N. 2002, in WE-Heraeus Seminar on Neutron Stars, Pulsars, and Supernova Remnants, ed. W. Becker, H. Lesch, & J. Trümper (Garching: MPE), 114

Lorimer, D. R., & Kramer, M. 2005, Handbook of Pulsar Astronomy (Cambridge: Cambridge Univ. Press)
Maggiore, M. 2000, Phys. Rep., 331, 283
McHugh, M. P., Zalamansky, G., Vernotte, F., & Lantz, E. 1996, Phys. Rev. D, 54, 5993
Navarro, J. F., Frenk, C. S., & White, S. D. M. 1997, ApJ, 490, 493
Nojiri, S., Odintsov, S. D., & Gorbunova, O. G. 2006, J. Phys. A, 39, 6627
Padmanabhan, T. 2005, in Proc. 29th Int. Cosmic Ray Conf. (Pune), 47
Patton, D. R. et al. 2002, ApJ, 565, 208
Sarangi, S., & Tye, S.-H. H. 2002, Phys. Lett. B, 536, 185
Sazhin, M. V. 1978, Soviet Astron., 22, 36
Sesana, A., Haardt, F., Madau, P., & Volonteri, M. 2004, ApJ, 611, 623
Silk, J., & Rees, M. J. 1998, A&A, 331, L1
Thorsett, S. E., & Dewey, R. J. 1996, Phys. Rev. D, 53, 3468
Vilenkin, A. 1981, Phys. Lett. B, 107, 47
Wyithe, J. S. B., & Loeb, A. 2003, ApJ, 590, 691